Journal of Machine Learning Research () Submitted ; Published

Training Highly Multiclass Classifiers

Maya R. Gupta MAYAGUPTA@GOOGLE.COM
Samy Bengio BENGIO@GOOGLE.COM
Google Inc.
1600 Amphitheatre Pkwy
Mountain View, CA 94301, USA

Jason Weston JWESTON@GOOGLE.COM
Google Inc.
76 9th Avenue,
New York, NY 10011 USA

Editor: Koby Crammer

Abstract

Classification problems with thousands or more classes often have a large range of class-confusabilities, and we show that the more-confusable classes add more noise to the empirical loss that is minimized during training. We propose an online solution that reduces the effect of highly confusable classes in training the classifier parameters, and focuses the training on pairs of classes that are easier to differentiate at any given time in the training. We also show that the adagrad method, recently proposed for automatically decreasing step sizes for convex stochastic gradient descent, can also be profitably applied to the non-convex joint training of supervised dimensionality reduction and linear classifiers as done in Wsabie. Experiments on ImageNet benchmark datasets and proprietary image recognition problems with 15,000 to 97,000 classes show substantial gains in classification accuracy compared to one-vs-all linear SVMs and Wsabie.

Keywords: large-scale, classification, multiclass, online learning, stochastic gradient

1. Introduction

Problems with many classes abound: from classifying a description of a flower as one of the over 300,000 known flowering plants (Paton et al., 2008), to classifying a whistled tune as one of the over 30 million recorded songs (Eck, 2013). Many practical multiclass problems are labelling images, for example face recognition, or tagging locations in vacation photos. In practice, the more classes considered, the greater the chance that some classes will be easy to separate, but that some classes will be highly confusable.

When training a discriminative multi-class classifier, the true goal is to minimize expected error on future samples, but in practice we minimize empirical error on samples we already have. In this paper, we show that classes that are more confusable add more noise to the empirical loss, making it a worse approximation to the expected error we wish to minimize. To address this, we propose minimizing a different approximation to the expected error that we term the *empirical class-confusion loss*. For the large-scale online training, we show that an *online empirical class-confusion loss* can be implemented for stochastic gradient descent by simply ignoring gradients corresponding to repeated confusions between

© Maya R. Gupta, Samy Bengio, and Jason Weston.

classes. This proposed strategy also automatically implements a form of *curriculum learning*, that is, of learning to distinguish easy classes before focusing on learning to distinguish hard classes (Bengio et al., 2009).

In this paper, we focus on classifiers that uses linear discriminant or a single prototypical feature vector to represent each sample. Linear classifiers are a popular approach to highly multiclass problems because they are efficient in terms of memory and inference and can provide good performance (Perronnin et al., 2012; Lin et al., 2011; Sanchez and Perronnin, 2011). Prototypes offer similar efficiency advantages. The last layer of a deep belief network classifier is often linear or soft-max discriminant functions (Bengio, 2009), and the proposed ideas for adapting online loss functions should be applicable in that context as well.

We apply the proposed adaptation to the multiclass linear classifier called Wsabie (Weston et al., 2011). We also simplify Wsabie's weighting of stochastic gradients, and employ a recent advance in automatic step-size adaptation called *adagrad* (Duchi et al., 2011). The resulting proposed Wsabie^{++} classifier almost doubles the classification accuracy on benchmark Imagenet datasets compared to Wsabie, and shows substantial gains over one-vs-all SVMs.

The rest of the article is as follows. After establishing notation in Section 2, we explain in Section 3 how different class confusabilities can distort the standard empirical loss. We then review loss functions for jointly training multiclass linear classifiers in Section 4, and stochastic gradient descent variants for large-scale learning in Section 5. In Section 6, we propose a practical online solution to adapt the empirical loss to account for the variance of class confusability. We describe our adagrad implementation in Section 7. Experiments are reported on benchmark and proprietary image classification datasets with 15,000-97,000 classes in Section 8 and 9. We conclude with some notes about the key issues and unresolved questions.

2. Notation And Assumptions

We take as given a set of training data $\{(x_t, \mathcal{Y}_t)\}$ for $t = 1, \ldots, n$, where $x_t \in \mathbb{R}^d$ is a feature vector and $\mathcal{Y}_t \subset \{1, 2, \ldots, G\}$ is the subset of the G class labels that are known to be correct labels for x_t. For example, an image might be represented by set of features x_t and have known labels $\mathcal{Y}_t = \{\texttt{dolphin}, \texttt{ocean}, \texttt{Half Moon Bay}\}$. We assume a discriminant function $f(x; \beta_g)$ has been chosen with class-specific parameters β_g for each class with $g = 1, \ldots, G$. The class discriminant functions are used to classify a test sample x as the class label that solves

$$\arg\max_g f(x; \beta_g). \tag{1}$$

Most of this paper applies equally well to "learning to rank", in which case the output might be a top-ranked or ranked-and-thresholded list of classes for a test sample x. For simplicity, we restrict our discussion and metrics to the classification paradigm given by (1).

Many of the ideas in this paper can be applied to any choice of discriminant function $f(x, \beta_g)$, but in this paper we focus on efficiency in terms of test-time and memory, and so we focus on class discriminants that are parameterized by a d-dimensional vector per class. Two such functions are: the inner product $f(x; \beta_g) = \beta_g^T x$, and the squared ℓ_2 norm $f(x; \beta_g) = -(\beta_g - x)^T(\beta_g - x)$. We also refer to these as linear discriminants and

Euclidean distance discriminants, respectively. For example, one-vs-all linear SVMs use a linear discriminant, where the β_g are each trained to maximize the margin between samples from the gth class and all samples from all other classes. The nearest means classifier (Hastie et al., 2001) uses an Euclidean distance discriminant where each class prototype β_g is set to be the mean of all the training samples labelled with class g. Both the linear and nearest-prototype functions produce linear decision boundaries between classes. And with either the linear or Euclidean discriminants, the classifier has a total of $G \times d$ parameters, and testing as per (1) scales as $O(Gd)$.

To reduce memory and test time, and also as a regularizer, it may be useful for the classifier to include a dimensionality reduction matrix (sometimes called an embedding matrix) $W \in \mathbb{R}^{m \times d}$, and then use linear or Euclidean discriminants in the reduced dimensionality space, e.g. $f(x; W, \beta_g) = \beta_g^T W x$ or $f(x; W, \beta_g) = -(\beta_g - x)^T W (\beta_g - x)$.

3. The Problem with a Large Variance in Class Confusability

The underlying goal when discriminatively training a classifier is to minimize expected classification error, but this goal is often approximated by the empirical classification errors on a given dataset. In this section, we show that the expected error does not count errors between confusable classes (like `dolphin` and `porpoise`) the same as errors between separable classes (like `cat` and `dolphin`), whereas the empirical error counts all errors equally. Consequently, more confusable classes add more noise to empirical error approximation of the expected error, and this confusable-class noise can adversely affect training.

Then in Section 6, we propose addressing this issue by changing the way we measure empirical loss to reduce the impact of errors between more-confusable classes.

3.1 Expected Classification Error Depends on Class Confusability

Define a classifier c as a map from an input feature vector x to a class such that $c : \mathbb{R}^d \to 1, 2, \ldots, G$. Let I be the indicator function, and assume there exists a joint probability distribution $P_{X,Y}$ on the random feature vector $X \in \mathbb{R}^d$ and class $Y \in \{1, 2, \ldots, G\}$. Then the expected classification error of classifier c is:

$$
\begin{aligned}
E_{X,Y}[I_{Y \neq c(X)}] &= E_X\left[E_{Y|X}[I_{Y \neq c(X)}]\right] && (2)\\
&= E_X\left[P_{Y|X}(Y \neq c(X))\right] \text{ because } I \text{ is a Bernoulli random variable} && (3)\\
&\approx \frac{1}{n}\sum_{t=1}^{n} P_{Y|x_t}(Y \neq c(x_t)), \text{law of large numbers approximation} && (4)\\
&\approx \frac{1}{n}\sum_{t=1}^{n} I_{y_t \neq c(x_t)}, && (5)
\end{aligned}
$$

where the approximation in (4) replaces the expectation with an average over n samples, an approximation that is asymptotically correct as $n \to \infty$ by the law of large numbers (LLN). The final approximation given in (5) produces the standard empirical error.

Equations (3) and (4) show that the expected error depends on the probability that a given feature vector x_t has corresponding random class label Y_t equal to the classifier's

decision $c(x_t)$. For example, suppose that sample x_t is equally likely to be class 1 or class 2, but no other class. If the classifier labels x_t as $c(x_t) = 1$, one should add $P_{Y|x_t}(Y \neq (c(x_t) = 1)) = 1/2$ to the approximate error given by (4). On the other hand, suppose that for another sample x_j, the probability of class 1 is .99 and the probability of class 3 is .01. Then if the classifier calls $c(x_j) = 1$ we should add $P_{Y|x_t}(Y \neq (c(x_t) = 1)) = .01$ to the loss, whereas if the classifier calls $c(x_j) = 3$ we should add $P_{Y|x_t}(Y \neq (c(x_t) = 1)) = .99$ to the loss. This relative weighting based on class confusions is in contrast to the standard empirical loss given in (5) that simply counts all errors equally.

One can interpret the standard empirical loss given in (5) as maximum likelihood approximation to (2) that estimates $P_{Y|x_t}$ given the training sample pair (x_t, y_t) as $\hat{P}_{Y|x_t}(y_t) = 1$ and $\hat{P}_{Y|x_t}(g) = 0$ for all other classes g. This maximum likelihood estimate converges asymptotically to (4), but for a finite number of training samples may produce a poor approximation. For binary classifiers, the approximation (5) may be quite good. We argue that (5) is generally a worse approximation as the number of classes increases. The key issue is that while the one-or-zero error approximation in (5) asymptotically converges to $P_{Y|x_t}$, it *converges more slowly* when classes are *more confusable*, and thus more-confusable classes add more "noise" to the approximation than less-confusable classes, biasing the empirical loss to overfit the noise of the more confusable class confusions.

Let us characterize this difference in noise. For any feature vector x and classifier c the true class label Y is a random variable, and thus the indicator $I_{Y \neq c(x_t)}$ in (5) is a random indicator with a binomial distribution with parameter $p = P_{Y|x_t}(Y \neq c(x_t))$. The variance of the random indicator $I_{Y \neq c(x_t)}$ is $p(1-p)$, and thus the more confusable the classes, the more variance there will be in the corresponding samples' contribution to the empirical loss.

Beyond noting the variance of the empirical errors is quadratic in p, it is not straightforward to formally characterize the distribution of the empirical loss for binomials with different p for finite n (see e.g. (Brown et al., 2001)). However we can emphasize this point with a histogram of simulated empirical errors in Fig. 1. The figure shows histograms of 1000 different simulations of the empirical error, calculated by averaging either 10 random samples (top) or 100 random samples (bottom) that either have $p = P_{Y|x_t}(Y \neq c(x_t)) = 0.5$ (left) or $p = P_{Y|x_t}(Y \neq c(x_t)) = 0.01$ (right).

The left-hand side of Fig. 1 corresponds to samples x that are equally likely to be one of two classes, and so even the Bayes classifier $c*$ is wrong half the time, such that $p = P_{Y|x_t}(Y \neq c(x_t)) = 0.5$. The empirical error of such samples will eventually converge to the true error 0.5, but we see (top left) that the empirical error of ten such samples varies greatly! Even hundred such samples (bottom left) are often a full .1 away from their converged value. This is in contrast to the right-hand examples corresponding to samples x_t that are easily classified such that $p = P_{Y|x_t}(Y \neq c(x_t)) = 0.01$. Their empirical error is generally much closer to the correct .01. Thus the more-confusable classes add more noise to the standard empirical loss approximation (5).

The standard empirical loss approximation (5) is exact in the special case that the Bayes error is zero and the classifier c is the Bayes classifier: then all classes are separable, and the classifier c perfectly separates them. For practical classification problems with many classes, we argue that at least some classes will be very confusable, and thus the Bayes error will not be zero, and (5) can be a dangerous approximation.

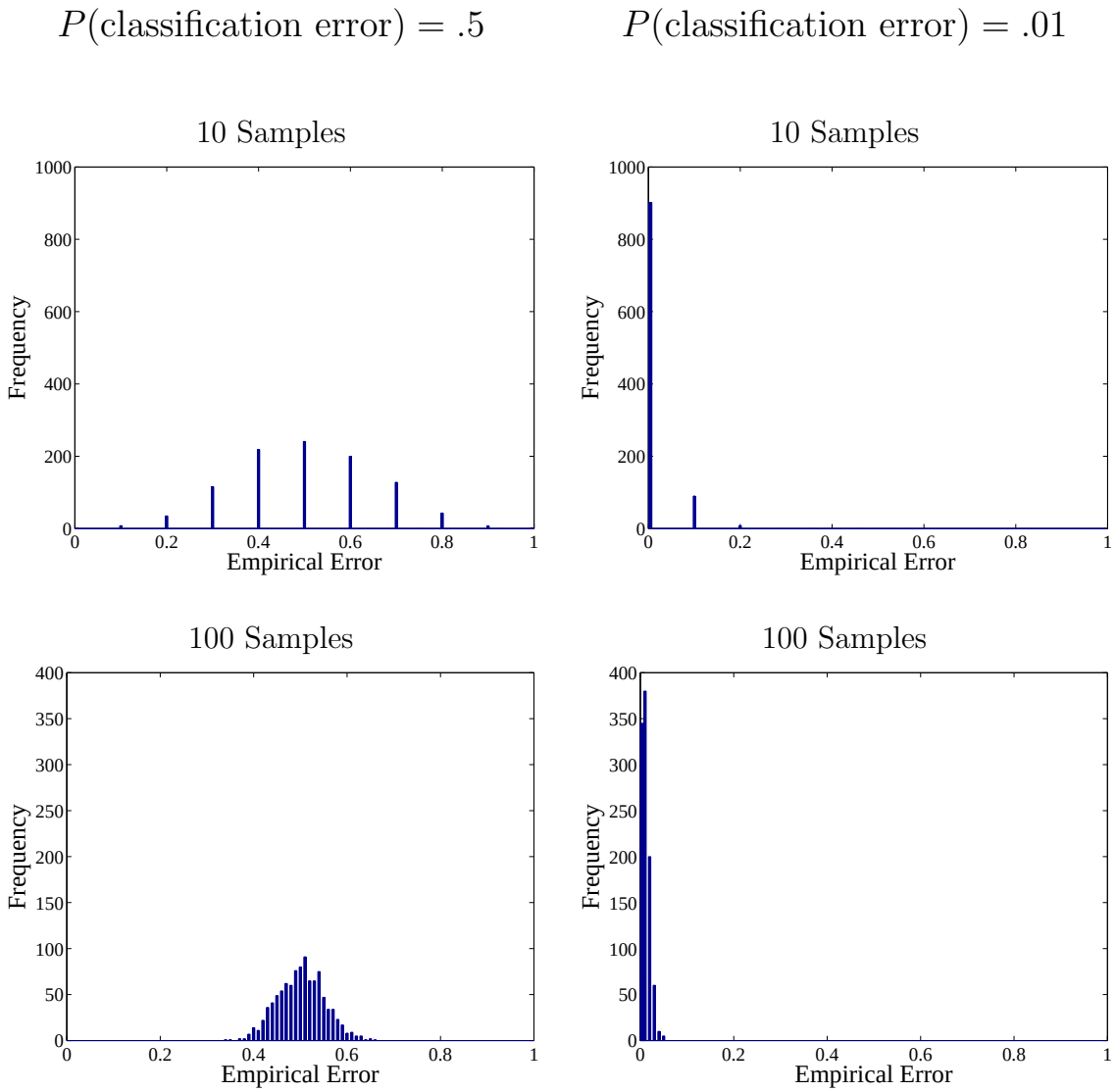

Figure 1: Histograms of the empirical error of 10 random samples (top) or 100 random samples (bottom). As the number of samples averaged grows, the empirical error will converge to the true probability of an error, either .5 (left) or .01 (right). But given a finite sample, the empirical error may be quite noisy, and when the true error is high (left) the empirical error can be much noisier than when the true error is low (right).

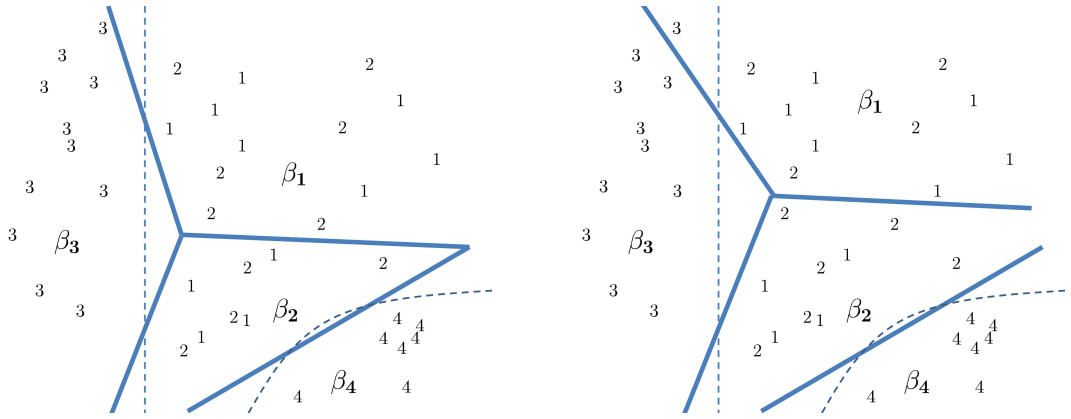

Empirical Errors: 10 Empirical Errors: 9

Figure 2: Two classifiers and the same draw of random training samples from four classes. Dotted lines correspond to the Bayes decision boundaries, and indicate that class 1 and class 2 are indistinguishable (same Bayes decision region). Solid lines correspond to the classifier decision boundaries, determined by which class prototype $\beta_1, \beta_2, \beta_3$, or β_4 is closest. The two figures differ in the placement of β_1, which produces different classifier decision boundaries. In this case, because of the randomness of the given training samples, the empirical error is higher for the left classifier than the right classifier, but the left classifier is closer to the optimal Bayes classifier.

Fig. 2 shows an example of empirical error being overfit to noise between confusable classes. The figure compares two classifiers. Each classifier uses a Euclidean discriminant function, that is, the gth class is represented by a prototype vector $\{\beta_g\}$, and a feature vector is classified as the nearest prototype with respect to Euclidean distance. Thus the decision boundaries are formed by the Voronoi diagram denoted with the thick lines, and the decision boundary between any two classes is linear.

The two classifiers in Fig. 2 differ only in the placement of β_1. One sees that decision boundaries produced are not independent of each other: the right classifier has moved β_1 up to reduce empirical errors between class 1 and class 2, but this also changes the decision boundary between classes 1 and 3, and incurs a new empirical error of a class 3 sample. The left classifier in Fig. 2 is actually closer to the Bayes decision boundaries (shown by the dotted lines), and would have lower error on a test set (on average).

If the feature dimension is high enough, then as the number of classes G grows, the number of decision boundaries between classes can grow at a worst-case rate of G^2, and yet the ability of these efficient classifiers to describe decision boundaries is fixed at Gd degrees of freedom. And with high-dimensional feature spaces, many classes are next to each other. This interdependence of the pairwise class decision boundaries is why simply minimizing the total empirical error is a bad strategy: it is too sensitive to the empirical error noise of the more-confusable classes.

3.2 Two Factors We Mostly Ignore In This Discussion

Throughout this paper we ignore the dependence of $P_{Y|x}(Y \neq c(x))$ on the particular feature vector x, and focus instead on how confusable a particular class $y = c(X)$ is averaged over X. For example, pictures of porpoises may on average be confused with pictures of dolphins, even though a particular image of a porpoise may be more or less confusable.

Also, we have thus far ignored the fact that discriminative training usually makes a further approximation of (5) by replacing the indicator by a convex approximation like the hinge loss. Such convex relaxations do not avoid the issues described in the previous section, though they may help. For example, the hinge loss increases the weight of an error that is made farther from the decision boundary. To the extent that classes are less confusable farther away from the decision boundary, the hinge loss may be a better approximation than the indicator to the probabilistic weighting of (4). However, if the features are high-dimensional, the distribution of distances from the decision boundary may be less variable than one would expect from two-dimensional intuition (see, e.g. (Hall and Marron, 2005)).

3.3 A Different Approximation for the Empirical Loss

We argued above that when computing the empirical test error, approximating $P_{Y|x_t}(Y \neq c(x_t))$ by 1 if $y_t = c(x_t)$ and by 0 otherwise adds preferentially more label noise from more confusable classes.

Here we propose a different approximation for $P_{Y|x_t}(Y \neq c(x_t))$. As usual, if $c(x_t) = y_t$, we approximate $P_{Y|x_t}(Y \neq c(x_t))$ by 0. But if $c(x_t) \neq y_t$, then we use the empirical probability that a training sample that has label y_t is not classified as $c(x_t)$:

$$P_{Y|x_t}(Y \neq c(x_t)) \approx E_{X|Y=y_t}\left[P(c(X) \neq c(x_t)\right] \tag{6}$$

$$\approx \left(\frac{\sum_{\tau=1}^{n} I_{y_\tau = y_t} I_{c(x_\tau) \neq c(x_t)}}{\sum_{\tau=1}^{n} I_{y_\tau = y_t}} \right) I_{y_t \neq c(x_t)}. \tag{7}$$

This approximation depends on how consistently feature vectors with training label y_t are classified as class $c(x_t)$, and counts common class-confusions less. For example, consider the right-hand classifier $c(x)$ in Fig. 2. There is just one training sample labeled `3` that is incorrectly classified as class `1`. The cost of that error according to (7) is 10/11, because there are eleven class `3` examples, and ten of those are classified as class `3`. On the other hand, the cost of incorrectly labeling a sample of class `1` as a sample of class `2` would be only 7/11, because seven of the eleven class `1` samples are not labeled as class `2`.

Thus this approximation generally has the desired effect of counting confusions between confusable classes relatively less than confusions between easy-to-separate classes. This approximation is more exact for "good" classifiers $c(x)$ that are more similar to the Bayes classifier, and more exact if the feature vectors X are equally predictive for each class label so that averaging over X in (6) is a good approximation for most realizations x_t.

One could implement this approximation in a sequential process: first train a classifier, then compute the empirical class-confusion probability matrix, and then re-train a classifier using the approximation (7) for the empirical loss. Shamir and Dekel (2010) proposed a

related but more extreme two-step approach for highly multi-class problems: first train a classifier on all classes, and then delete classes that are poorly estimated by the classifier.

In this paper we go to the other extreme, we next propose continuously evolving the classifier to ignore the currently highly-confusable classes by implementing (6) in an online fashion with SGD. This simple variant can be interpreted as implementing curriculum learning (Bengio et al., 2009), a topic we discuss further in Section 6.2.1. But before detailing the proposed online strategy in Section 6, we need to review related work in loss functions for multi-class classifiers.

4. Related Work in Loss Functions for Multiclass Classifiers

In this section, we review loss functions for multiclass classifiers, and discuss recent work adapting such loss functions to the online setting for large-scale learning.

One of the most popular classifiers for highly multiclass learning is one-vs-all linear SVMs, which have only $O(Gd)$ parameters to learn and store, and $O(Gd)$ time needed for testing. A clear advantage of one-vs-all is that the G class discriminant functions $\{f_g(x)\}$ can be trained independently. An alternate parallelizable approach is to train all G^2 one-vs-one SVMs, and let them vote for the best class (also known as round-robin and all-vs-all). Binary classifiers can also be combined using error-correcting code approaches (Dietterich and Bakiri, 1995; Allwein et al., 2000; Crammer and Singer, 2002). A well-regarded experimental study of multiclass classification approaches by Rifkin and Klatau (2004) showed that one-vs-all SVMs performed "just as well" on a set of ten benchmark datasets with 4-49 classes as one-vs-one or error-correcting code approaches.

A number of researchers have independently extended the two-class SVM optimization problem to a joint multiclass optimization problem that maximizes pairwise margins subject to the training samples being correctly classified, with respect to pairwise slack variables (Vapnik, 1998; Weston and Watkins, 1998, 1999; Bredensteiner and Bennet, 1999)[1]. These extensions have been shown to be essentially equivalent quadratic programming problems (Guermeur, 2002). The minimized empirical loss can be stated as the sum of the pairwise errors:

$$L_{\text{pairwise}}(\{\beta_g\}) = \sum_{t=1}^{n} \quad \frac{1}{|\mathcal{Y}_t|} \sum_{y^+ \in \mathcal{Y}_t} \frac{1}{|\mathcal{Y}_t^C|} \quad \sum_{y^- \in \mathcal{Y}_t^C} |b - f(x_t; \beta_{y^+}) + f(x_t; \beta_{y^-})|_+, \qquad (8)$$

where $|\cdot|_+$ is short-hand for $\max(0, \cdot)$, b is a margin parameter, $\mathcal{Y}_t^C$ is the complement set of $\mathcal{Y}_t$, and we added normalizers to account for the case that a given x_t may have more than one positive label such that $|\mathcal{Y}_t| > 1$.

Crammer and Singer (2001) instead suggested taking the maximum hinge loss over all the negative classes:

$$L_{\text{max loss}}(\{\beta_g\}) = \sum_{t=1}^{n} \quad \frac{1}{|\mathcal{Y}_t|} \sum_{y^+ \in \mathcal{Y}_t} \quad \max_{y^- \in \mathcal{Y}_t^C} |b - f(x_t; \beta_{y^+}) + f(x_t; \beta_{y^-})|_+. \qquad (9)$$

1. See also the work of Herbrich et al. (2000) for a related pairwise loss function for ranking rather than classification.

This maximum hinge-loss is sometimes called *multiclass SVM*, and can be derived from a margin-bound (Mohri et al., 2012). Daniely et al. (2012) theoretically compared multiclass SVM with one-vs-all, one-vs-one, tree-based linear classifiers and error-correcting output code linear classifiers. They showed that the hypothesis class of multiclass SVM contains that of one-vs-all and tree-classifiers, which strictly contain the hypothesis class of one-vs-one classifiers. Thus the potential performance with multiclass SVM is larger. However they also showed that the approximation error of one-vs-one is smallest, with multiclass SVM next smallest.

Statnikov et al. (2005) compared eight multiclass classifiers including that of Weston and Watkins (1999) and Crammer and Singer (2001) on nine cancer classification problems with 3 to 26 classes and less than 400 samples per problem. On these small-scale datasets, they found the Crammer and Singer (2001) classifier was best (or tied) on 2/3 of the datasets, and the pairwise loss given in (8) performed almost as well.

Lee et al. (2004) prove in their Lemma 2 that previous approaches to multiclass SVMs are not guaranteed to be asymptotically consistent. (For more on consistency of multiclass classification loss functions, see Rifkin and Klatau (2004), Tewari and Bartlett (2007), Zhang (2004), and Mroueh et al. (2012)). Lee et al. (2004) proposed a multiclass loss function that is consistent. They force the class discriminants to sum to zero such that $\sum_g f(x;\beta_g) = 0$ for all x, and define the loss:

$$L_{\text{total loss}}(\{\beta_g\}) = \sum_{t=1}^{n} \sum_{y^- \in \mathcal{Y}_t^C} |f(x_t;\beta_{y^-}) - \frac{1}{G-1}|_+. \tag{10}$$

This loss function jointly trains the class discriminants so that the total sum of wrong class discriminants for each training sample is small. Minimizing this loss can be expressed as a constrained quadratic program. The experiments of Lee et al. (2004) on a few small datasets did not show much difference between the performance of (10) and (8).

5. Online Loss Functions for Training Large-scale Multiclass Classifiers

If there are a large number of training samples n, then computing the loss for each candidate set of classifier parameters becomes computationally prohibitive. The usual solution is to minimize the loss in an online fashion with stochastic gradient descent, but exactly how to sample the stochastic gradients becomes a key issue. Next, we review two stohastic gradient approaches that correspond to different loss functions: AUC sampling (Grangier and Bengio, 2008) and WARP sampling (used in the Wsabie classifier) (Weston et al., 2011).

5.1 AUC Sampling

For a large number of training samples n, Grangier and Bengio (2008) proposed optimizing (8) by sequentially uniformly sampling from each of the three sums in (8):

1. draw one training sample x_t,
2. draw one correct class y^+ from $\mathcal{Y}_t$, and
3. draw one incorrect class y^- from $\mathcal{Y}_t^C$,

4. compute the corresponding stochastic gradient of the loss in (8),

5. update the classifier parameters.

This sampling strategy, referred to as *area under the curve* (AUC) *sampling*, is inefficient because most randomly drawn incorrect class samples will have zero hinge loss and thus not produce an update to the classifier.

5.2 WARP Sampling

The *weighted approximately ranked pairwise* (WARP) sampling was introduced by Weston et al. (2011) to make the stochastic gradient sampling more efficient than AUC sampling, and was evolved from the weighted pairwise classification loss of Usunier et al. (2009). Unlike AUC sampling, WARP sampling focuses on sampling from negative classes that produce non-zero stochastic gradients for a given training example.

To explain WARP sampling, we first define the *WARP loss*:

$$L_{\text{WARP}}(\{\beta_g\}) = \sum_{t=1}^{n} \quad \frac{1}{|\mathcal{Y}_t|} \sum_{y^+ \in \mathcal{Y}_t} \quad \frac{1}{|\mathcal{V}_{t,y^+}|} \sum_{y^v \in \mathcal{V}_{t,y^+}} w(y^+) \quad |b - f(x_t; \beta_{y^+}) + f(x_t; \beta_{y^v})|_+ \tag{11}$$

where $w(y^+)$ is a weight on the correct label, and $\mathcal{V}_{t,y^+}$ is the set of *violating classes* defined:

$$\mathcal{V}_{t,y^+} = \{y^v \text{ s.t. } |b - f(x_t; \beta_{y^+}) + f(x_t; \beta_{y^v})|_+ > 0\}. \tag{12}$$

As in Usunier et al. (2009), Weston et al. (2011) suggest using a weight function $w(y^+)$ that is an increasing function of the number of violating classes. Because the number of violating classes defines the rank of the correct class y^+, they denote the number of violating classes for a training sample with training class y^+ as $r(y^+)$. They suggest using the truncated harmonic series for the weight function,

$$w(y^+) = \sum_{j=1}^{r(y^+)} \frac{1}{j}. \tag{13}$$

Weston et al. (2011) propose *WARP sampling* which sequentially uniformly samples from each of the three sums in (11):

1. draw one training sample x_t,

2. draw one correct class y^+ from $\mathcal{Y}_t$, and

3. draw one violating class y^v from $\mathcal{V}_{t,y^+}$ if one exists,

4. compute the corresponding stochastic gradient of the loss in (8)

5. update the classifier parameters.

To sample a violating class from $\mathcal{V}_{t,y^+}$, the negative classes in $\mathcal{Y}_t^C$ are uniformly randomly sampled until a class that satisfies the violation constraint (12) is found, or the number of allowed such trials (generally set to be G) is exhausted. The rank $r(y^+)$ needed to calculate the weight in (13) is estimated to be $(G-1)$ divided by the number of negative classes $y^- \in \mathcal{Y}_t$ that had to be tried before finding a violating class y^v from $\mathcal{V}_{t,y^+}$.

5.3 Some Notes Comparing AUC and WARP Loss

We note that WARP sampling is more likely than AUC sampling to update the parameters of a training sample's positive class y^+ if y^+ has few violating classes, that is if (x_t, y_t) is already highly-ranked by (1). Specifically, suppose a training pair (x_t, y_t) is randomly sampled, and suppose $H > 0$ of the G classes are violators such that their hinge-loss is non-zero with respect to (x, y^+). WARP sampling will draw random classes until it finds a violator and makes an update, but AUC will only make an update if the one random class it draws happens to be a violator, so only $H/(G-1)$ of the time. By definition, the higher-ranked the correct class y_t is for x_t, the smaller the number of violating classes H, and the less likely AUC sampling will update the classifier to learn from (x_t, y_t).

In this sense, WARP sampling is more focused on fixing class parameters that are almost right already, whereas AUC sampling is more focused on improving class parameters that are very wrong. At test time, classifiers choose only the highest-ranked class discriminant as a class label, and thus the fact that AUC sampling updates more often on lower-ranked classes is likely the key reason that WARP sampling performs so much better in practice (see the experiments of (Weston et al., 2011) and the experiments in this paper). Even in ranking, it is usually only the top ranked classes that are of interest. However, the WARP weight $w(y^+)$ given in (13) partly counteracts this difference by assigning greater weights (equivalently a larger step-size to the stochastic gradient) if the correct class has many violators, as then its rank is lower. In this paper, one of the proposals we make is to use constant weights $w(y^+) = 1$, so the sampling is more focused on improving classes that are already highly-ranked.

AUC sampling is also inefficient because so many of the random samples result in a zero gradient. In fact, we note that the probability that AUC sampling will update the classifier *decreases* if there are more classes. Specifically, suppose for a given training sample pair (x_t, y_t) there are H classes that violate it, and that there are G classes in total. Then the probability that AUC sampling updates the classifier for (x_t, y_t) is $H/(G-1)$, which linearly decreases as the number of classes G is increased.

5.4 Online Versions of Other Multiclass Losses

WARP sampling implements an online version of the pairwise loss given in (8) (Weston et al., 2011). One can also interpret the WARP loss sampling as an online approximation of the maximum hinge loss given in (9), where the maximum violating class is approximated by the sampled violating class. This interpretation does not call for a rank-based weighting $w(y^+)$, and in fact we found that setting $w(y^+) = 1$ improved accuracy by roughly 20% on a large-scale image annotation task (see Table 6). A better approximation of (9) would require sampling multiple violating classes and then taking the class with the worst discriminant, we did not try this due to the expected time needed to find multiple violating classes. Further, we hypothesize that choosing the class with the largest violation as the violating class could actually perform poorly for practical highly multiclass problems like Imagenet because the worst discriminant may belong to a class that is a missing correct label, rather than an incorrect label.

An online version of the loss proposed by Lee et al. (2004) and given in (10) would be more challenging to implement because the G class discriminants are required to be normalized; we do not know of any such experiments.

5.5 The Wsabie Classifier

Weston et al. (2011) combined the WARP sampling with online learning of a supervised linear dimensionality reduction. They learn an embedding matrix $W \in \mathbb{R}^{m \times d}$ that maps a given d-dimensional feature vector x to an m-dimensional "embedded" vector $Wx \in \mathbb{R}^m$, where $m \leq d$, and then the G class-specific discriminants of dimension m are trained to separate classes in the embedding space. Weston et al. (2011) referred to this combination as the *Wsabie* classifier. This changes the WARP loss given in (11) to the non-convex Wsabie loss, defined:

$$L_{\text{Wsabie}}(W, \{\beta_g\}) = \sum_{t=1}^{n} \sum_{y^+ \in \mathcal{Y}_t} \sum_{y^v \in \mathcal{V}_{t,y^+}} w(y^+) \quad |b - f(Wx_t; \beta_{y^+}) + f(Wx_t; \beta_{y^v})|_+.$$

Adding the embedding matrix W changes the number of parameters from Gd to $Gm + md$. For a large number of classes G and a small embedding dimension m (the case of interest here) this reduces the overall parameters, and so the addition of the embedding matrix W acts as a regularizer, reduces memory, and reduces testing time.

6. Online Adaptation of the Empirical Loss to Reduce Impact of Highly Confusable Classes

In this section, we present a simple and memory-efficient online implementation of the empirical class-confusion loss we proposed in Section 3.3 that reduces the impact of highly confusable classes on the standard empirical loss. First, we describe the batch variant of this proposal and quantify its effect. Then in Section 6.2 we describe a sampling version. In Section 6.3, we propose a simple extension that experimentally increases the accuracy of the resulting classifier, without using additional memory. We show the proposed online strategy works well in practice in Section 9.

6.1 Reducing the Effect of Highly Confusable Classes By Ignoring Last Violators

We introduce the key idea of a *last violator* class with a simple example before a formal definition. Suppose during online training the hundreth training sample x_{100} has label $y_{100} = \texttt{tiger}$, and that the last training sample we saw labelled `tiger` was x_5. And suppose `lion` was a violating class for that training sample pair $(x_5, \texttt{tiger})$, that is $|1 - f(x_5; \theta_{\texttt{tiger}}) + f(x_5; \theta_{\texttt{lion}})|_+ > 0$. Then for sample $(x_{100}, \texttt{tiger})$ we call the class `lion` the *last violator class*.

Formally, we call class v_{t,y^+} a *last violator* for the training sample pair (x_t, y^+) if x_τ was the last training sample for which y^+ was the sampled positive class and v_{t,y^+} was a violator for (x_τ, y^+), that is, $v_{t,y^+} \in \mathcal{V}_{\tau,y^+}$. The *set of violators* $\mathcal{V}_{\tau,y^+}$ becomes the *set of last violators of* (x_t, y^+), which we denote $\tilde{\mathcal{V}}_{t,y^+}$.

In order to decrease the effect of highly confusable classes on training the classifier, we propose to ignore losses for any violator class that was also a last violator class. The reasoning is that if the last violator class and a current violator class are the same, it indicates that the class y_t and that violator class are consistently confused (e.g. `tiger` and `lion`). And if two classes are consistently confused, we would like to reduce their impact on the empirical loss, as discussed in Section 3.

For example, say sequential training samples that were labelled `cat` had the following violating classes:

`dog` and `pig`, `dog` and `pig`, none, `dog`, `dog`, none, `dog`, pig.

The proposed approach ignores any violator was also a last violator:

`dog` and `pig`, ~~`dog`~~ and ~~`pig`~~, none, `dog`, ~~`dog`~~, none, `dog`, `pig`.

Mathematically, to ignore last violators we simply add an indicator function $\mathbb{I}$ to the loss function. For example, ignoring last violators with the WARP loss from (11) can be written:

$$L_{\text{proposed}}(\{\theta_g\}) = \sum_{t=1}^{n} \sum_{y^+ \in \mathcal{Y}_t} \sum_{y^v \in \mathcal{V}_{t,y^+}} w(y^+) \quad |b - f(x_t;\theta_{y^+}) + f(x_t;\theta_{y^v})|_+ \quad \mathbb{I}_{y^v \notin \tilde{\mathcal{V}}_{t,y^+}}. \tag{14}$$

That is, instead of forming one estimate of the correct empirical loss as we proposed in Section 3.3, here we approximate the correct empirical loss as the average of the series of Bernoulli random variables represented by the extra indicator in (14). In fact, the proposal to ignore last violators implements the proposed approximation (7): the probability that an error is not-counted is the probability that the violating class is confused with the training class:

Proposition 1: Suppose there are n samples labelled class g, and each such sample has probability p of being classified as class h. Then the expected number of losses summed in (11) is np, but the expected number of losses summed in (14) is $(n-1)p(1-p)+p$.

This reduction of the empirical error from np to $np(1-p)$ is the same as in the earlier proposal (6), where in Proposition 1 the probability $1-p$ is the same as the expectation in (6).

6.2 Ignoring Sampled Last Violators for Online Learning

Building on the WARP sampling proposed by Weston et al. (2011) and reviewed in Section 5.2, we propose an online sampling implementation of (14), where for each class y^+ we store one sampled last violator and only update the classifier if the current violator is not the same as the last violator. Specifically,

1. draw one training sample x_t,
2. draw one correct class y^+ from $\mathcal{Y}_t$,

3. if there is no last violator v_{t,y^+} or if v_{t,y^+} exists but is not a violator for (x_t, y^+), then draw and store one violating class y^v from $\mathcal{V}_{y^+}$ and

   (a) compute the corresponding stochastic gradient of the loss in (8)

   (b) update the parameters.

Table 1 re-visits the same example as earlier, and illustrates for eight sequential training examples whose training label was `cat` what the last violator class is, whether the last violator is a current violator (n which case the current error is ignored), or if not ignored, which of the current violators is randomly sampled for the classifier update.

Throughout the training, the state of the sampled last violator for any class y^+ can be viewed as a Markov chain. We illustrate this for the class y^+ and two possible violating classes g and h in Fig. 3.

In the experiments to follow, we couple the proposed online empirical class-confusion loss sampling strategy with an embedding matrix as in the Wsabie algorithm for efficiency and regularization, and refer to this as Wsabie^{++}. A complete description of Wsabie^{++} is given in Table 3, including the adagrad stepsize updates described in the next section. The memory needed to implement this discounting is $O(G)$ because only one last violator class is stored for each of the G classes.

Set of `Cat` Violators	`Cat`'s LV	`Cat`'s LV Violates?	New Violator Sampled?
1: `dog` and `pig`	none	-	`dog`
2: `dog` and `pig`	`dog`	yes	ignored
3: `dog`	`dog`	yes	ignored
4: `dog` and `pig`	`dog`	yes	ignored
5: `pig`	`dog`	no	`pig`
6: no violators	`pig`	no	none
7: `dog`	none	-	`dog`
8: `dog`	`dog`	yes	ignored

Table 1: Example of ignoring sampled last violators for eight sequential samples (one per row) whose training label is `cat`.

6.2.1 Curriculum Learning

We have primarily motivated ignoring last violators as a better approximation for the expected classification error. However, because this approach is online, it has a second practical effect of changing the distribution of classifier updates as the classifier improves during training. Consider the classifier at some fixed point during training. At that point, classes that are better separated from all other classes are less likely to have a last violator stored, and thus more likely to be trained on. This increases the chance that the classifier first learns to separate easy-to-separate classes. At each point in time, the classifier is less likely to be updated to separate classes it finds most confusable. Bengio et al. (2009) have argued that this kind of easy-to-hard learning is natural and useful, particularly when optimizing

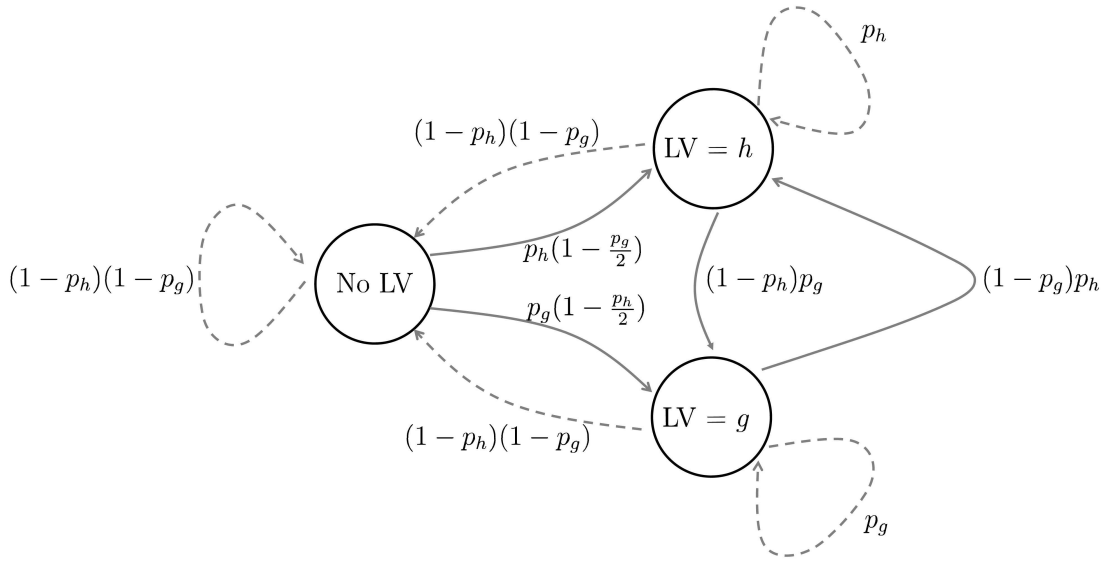

Figure 3: In the proposed sampling strategy for the online empirical class-confusion loss, the state of the last violator (LV) for a class y^+ can be interpreted as a Markov chain where a transition occurs for each training sample. The figure illustrates the case where there are just two possible violating classes, class g and class h, which violate samples of class y^+ with probability p_g and p_h respectively. Then the last violator for class y^+ is always in one of three possible states: no last violator, class h is the last violator, or class g is the last violator. Solid lines indicate a violation that is counted; dotted lines indicate a violation that is ignored. The three states have stationary distribution:

$$
\begin{aligned}
P(\text{No LV}) &= \frac{1}{Z}, \\
P(\text{LV } = g) &= \frac{1}{Z}\frac{p_g(2+p_h-p_gp_h)}{2(p_g-1)(p_gp_h-1)}, \\
P(\text{LV } = h) &= \frac{1}{Z}\frac{p_h(2+p_g-p_gp_h)}{2(p_h-1)(p_gp_h-1)},
\end{aligned}
$$

where Z is the normalizer that makes the stationary distribution sum to 1.

True Class		Last Violator Class
`tiger`	$\rightarrow$	`lion`
`lion`	$\rightarrow$	`cat`
`cat`	$\rightarrow$	`kitten`
`kitten`	$\rightarrow$	`panther`
`panther`	$\rightarrow$	`cat`

Table 2: Example chain of five classes and their sampled last violator.

non-convex loss functions as is the case when one jointly learns an embedding matrix W for efficiency and regularization.

6.3 Extending the Discounting Loss to Multiple Last Violators

Table 2 shows an example of five classes and what their last violator class might be at some point in the online training. For example, Table 2 suggests that `tiger` and `lion` are highly confusable, and that `lion` and `cat` are highly confusable, and thus we suspect that `tiger` and `cat` may also be highly confusable. To further reduce the impact of these sets of highly confusable classes, we extend the above approach to ignoring a training sample if it is currently violated by its last violator class's last violator class, and so on. The longer the chain of last violators we choose to ignore, the more training samples are ignored, and the ignored training samples are preferentially those belonging to clusters of classes that are highly-confusable with each other.

Formally, let v^2_{t,y^+} denote the last violator of the last violator of y^+, that is $v^2_{t,y^+} = v_{t,v_{t,y^+}}$. For the example given in Table 2, if y^+ is `tiger`, then its last violator is $v_{t,y^+} =$ `lion`, and $v^2_{t,y^+} =$ `cat`. More generally, let v^Q_{t,y^+} be the Qth-order last violator, for example $v^3_{t,\texttt{tiger}} =$ `kitten`.

Let $\tilde{\mathcal{V}}^Q_{t,y^+}$ be the set of last violators up through order Q for positive class y^+ and the tth sample. We extend (14) to ignore this larger set of likely highly-confusable classes:

$$L_{\text{proposed-}Q}(\{\theta_g\}) = \sum_{t=1}^{n} \sum_{y^+ \in \mathcal{Y}_t} \sum_{y^v \in \mathcal{V}_{t,y^+}} |b - f(x_t; y^+) + f(x_t; y^v)|_+ \quad \mathbb{I}_{y^v \notin \tilde{\mathcal{V}}^Q_{t,y^+}}. \qquad (15)$$

To use (15) in an online setting, each time a training sample and its positive class are drawn, we check if any q-th order last violator v^q_{t,y^+} for any $q \leq Q$ is a current violator, and if so, we ignore that training sample and move directly to the next training sample without updating the classifier parameters.

Table 3 gives the complete proposed sampling and updating algorithm for Euclidean discriminant functions, including the adaptive adagrad step-size explained in Section 7 which follows. For Euclidean discriminant functions we did not find (experimentally) that we needed any constraints or additional regularizers on W or $\{\beta_g\}$, though if desired a regularization step can be added.

7. Adagrad For Learning Rate

Convergence speed of stochastic gradient methods is sensitive to the choice of stepsizes. Recently, Duchi et al. (2011) proposed a parameter-dependent learning rate for stochastic gradient methods. They proved that their approach has strong theoretical regret guarantees for convex objective functions, and experimentally it produced better results than comparable methods such as regularized dual averaging (Xiao, 2010) and the passive-aggressive method (Crammer et al., 2006). In our experiments, we applied adagrad both to the convex training of the one-vs-all SVMs and AUC sampling, as well as to the non-convex Wsabie^{++} training. Inspired by our preliminary results using adagrad for non-convex optimization, Dean et al. (2012) also tried adagrad for non-convex training of a deep belief network, and also found it produced substantial improvements in practice.

The main idea behind adagrad is that each parameter gets its own stepsize, and each time a parameter is updated its stepsize is decreased to be proportional to the running sum of the magnitude of all previous updates. For simplicity, we limit our description to the case where the parameters being optimized are unconstrained, which is how we implemented it. For memory and computational efficiency, Duchi et al. (2011) applying adagrad separately for each parameter (as opposed to modeling correlations between parameters).

We applied adagrad to adapt the stepsize for the G classifier discriminants $\{\beta_g\}$ and the $m \times d$ embedding matrix W. We found that we could save memory without affecting experimental performance by averaging the adagrad learning rate over the embedding dimensions such that we keep track of one scalar adagrad weight per class. That is, let $\Delta_{g,\tau}$ denote the stochastic gradient for β_g at time τ, then we update β_g as follows:

$$\beta_{g,t+1} = \beta_{g,t} - \eta \left(\sum_{\tau=0}^{t} \left(\frac{\Delta_{\tau,g}^T \Delta_{\tau,g}}{d} \right) \right)^{-1/2} \Delta_{g,\tau}. \tag{16}$$

Analogously, we found it experimentally effective and more memory efficient to keep track of one averaged scalar adagrad weight for each of the m rows of the embedding matrix W.

There are two main effects to using adagrad. First, suppose there are two classes that are updated equally often, then the class with larger stochastic gradients $\{\Delta_\tau\}$ will experience a faster-decaying learning rate. Second, and we believe the more relevant issue for our use, is that some classes are updated frequently, and some classes rarely. Suppose that all stochastic gradients $\{\Delta_\tau\}$ have the same magnitude, then the classes that are updated more rarely experience relatively larger updates. In our experiments the second effect was predominant, which we tested by setting the learning rate for each parameter proportaionl to the inverse square root of the number of times that parameter has been updated. This "counting adagrad" produced results that were not statistically different using (16). (The experimental results in this paper are reported using adagrad proper as per (16).)

We use α to refer to the running sum of gradient magnitudes in the complete Wsabie^{++} algorithm description given in Table 3.

Model:

Training Data Pairs: $(x_t, \mathcal{Y}_t)$ for $t = 1, 2, \ldots, n$
Embedded Euclidean Discriminant: $f(Wx; \beta_g) = -(\beta_g - Wx)^T(\beta_g - Wx)$

Hyperparameters:

Stepsize: $\lambda \in \mathbb{R}_+$
Margin: $b \in \mathbb{R}_+$
Depth of last violator chain: $Q \in \mathbb{N}$

Initialize:

$W_{j,r}$ set randomly to -1 or 1 for $j = 1, 2, \ldots, m$, $r = 1, 2, \ldots, d$
$\beta_g = \mathbf{0}$ for all $g = 1, 2, \ldots, G$
$\alpha_g = \mathbf{0}$ for all $g = 1, 2, \ldots, G$
$\alpha_{W_j} = \mathbf{0}$ for all $j = 1, 2, \ldots, m$
v_{y^+} = empty set for all y^+

While Not Converged:

Sample x_t uniformly from $\{x_1, \ldots, x_n\}$.
Sample y^+ uniformly from $\mathcal{Y}_t$.
If $|b - f(Wx_t; \beta_{y^+}) + f(Wx_t; \beta_{v^q_{y^+}})|_+ > 0$ for any $q = 1, 2, \ldots, Q$, **continue**.
Set foundViolator = false.
For count = 1 to G:
Sample y^- uniformly from $\mathcal{Y}_t^C$.
If $|b - f(Wx_t; \beta_{y^+}) + f(Wx_t; \beta_{y^-})|_+ > 0$,
set foundViolator = true and **break**.
If foundViolator = false, set v_{y^+} to the empty set and **continue**.
Set $v_{y^+} = y^-$.
Compute the stochastic gradients:

$$\Delta_{y^+} = 2(\beta_{y^+} - Wx_t)$$
$$\Delta_{y^-} = -2(\beta_{y^-} - Wx_t)$$
$$\Delta_W = (\beta_{y^-} - \beta_{y^+})(Wx_t)^T.$$

Update the adagrad parameters:

$$\alpha_{y^+} = \alpha_{y^+} + \tfrac{1}{d}\Delta_{y^+}^T\Delta_{y^+}$$
$$\alpha_{y^-} = \alpha_{y^-} + \tfrac{1}{d}\Delta_{y^-}^T\Delta_{y^-}$$
$$\alpha_{W_j} = \alpha_{W_j} + \tfrac{1}{d}\Delta_{W_j}^T\Delta_{W_j} \text{ for } j = 1, 2, \ldots, m.$$

Update the classifier parameters:

$$\beta_{y^+} = \beta_{y^+} - \frac{\lambda}{\sqrt{\alpha_{y^+}}}\Delta_{y^+}$$
$$\beta_{y^-} = \beta_{y^-} - \frac{\lambda}{\sqrt{\alpha_{y^-}}}\Delta_{y^-}$$
$$W_j = W_j - \frac{\lambda}{\sqrt{\alpha_{W_j}}}\Delta_{W_j} \text{ for } j = 1, 2, \ldots, m.$$

Table 3: Wsabie^{++} Training (For Euclidean Discriminants)

8. Experiments

We first detail the datasets used. Then in Section 8.2 we describe the features. In Section 8.3 we describe the different classifiers compared and how the parameters and hyperparameters were set.

8.1 Datasets

Experiments were run with four datasets, as summarized in Table 4 and detailed below.

	16k ImageNet	22k ImageNet	21k Web Data	97k Web Data
Number of Classes	15,589	21,841	21,171	96,812
Number of Samples	9 million	14 million	9 million	40 million
Number of Features	1024	479	1024	1024

Table 4: Datasets

8.1.1 ImageNet Datasets

ImageNet (Deng et al., 2009) is a large image dataset organized according to WordNet (Fellbaum, 1998). Concepts in WordNet, described by multiple words or word phrases, are hierarchically organized. ImageNet is a growing image dataset that attaches one of these concepts to each image using a quality-controlled human-verified labeling process.

We used the spring 2010 and fall 2011 releases of the Imagenet dataset. The spring 2010 version has around 9M images and 15,589 classes (16k ImageNet). The *fall 2011* version has about 14M images and 21,841 classes (22k ImageNet). For both datasets, we separated out 10% of the examples for validation, 10% for test, and the remaining 80% was used for training.

8.1.2 Web Datasets

We also had access to a large proprietary set of images taken from the web, together with a noisy annotation based on anonymized users' click information. We created two datasets from this corpus that we refer to as 21k Web Data and 97k Web Data. The 21k Web Data contains about 9M images, divided into 20% for validation, 20% for test, and 60% for train, and the images are labelled with 21,171 distinct classes. The 97k Web Data contains about 40M images, divided into 10% for validation, 10% for test, and 80% for train, and the images are labelled with 96,812 distinct classes.

There are five main differences between the Web Data and ImageNet. First, the types of labels found in Imagenet are more *academic*, following the strict structure of WordNet. In contrast, the Web Data labels are taken from a set of popular queries that were the input to a general-purpose image search engine, so it includes people, brands, products, and abstract concepts. Second, the number of images per label in Imagenet is artificially forced to be somewhat uniform, while the Web Data distribution of number of images per label is generated by popularity with users, and is thus more exponentially distributed. Third, because of the popular origins of the Web datasets, classes may be translations of each other, plural vs. singular concepts, or synonyms (for examples, see Table 7). Thus

we expect more highly-confusable classes for the Web Data than ImageNet. A fourth key difference is Imagenet disambiguates polysemyous labels whereas Web Data does not, for example, an image labeled `palm` might look like the palm of a hand or like a palm tree. The fifth difference is that there may be multiple given positive labels for some of the Web samples, for example, the same image might be labelled `mountain`, `mountains`, `Himalaya`, and `India`.

Lastly, classes may be at different and overlapping precision levels, for example the class `cake` and the class `wedding cake`.

8.2 Features

We do not focus on feature extraction in this work, although features certainly can have a big impact on performance. For example, Sanchez and Perronnin (2011) recently achieved a 160% gain in accuracy on the 10k ImageNet datatset by changing the features but not the classification method.

In this paper we use features, similar to those used in Weston et al. (2011). We first combined multiple spatial (Grauman and Darrell, 2007) and multiscale color and texton histograms (Leung and Malik, 1999) for a total of about 5×10^5 dimensions. The descriptors are somewhat sparse, with about 50000 non-zero weights per image. Some of the constituent histograms are normalized and some are not. We then perform kernel PCA (Schoelkopf et al., 1999) on the combined feature representation using the intersection kernel (Barla et al., 2003) to produce a 1024-dimensional or 479-dimensional input vector per image (see Tab. 4), which is then used as the feature vectors for the classifiers.

8.3 Classifiers Compared and Hyperparameters

We experimentally compared the following linear classifiers: nearest means, one-vs-all SVMs, AUC, Wsabie, and the proposed Wsabie^{++} classifiers. Table 5 compares these methods as they were implemented for the experiments.

	One-vs-all SVMs 1+:1-	One-vs-all SVMs	AUC Sampling	Wsabie	Wsabie^{++}
Loss Function	separable	separable	pairwise	pairwise	pairwise
Regularization	ℓ_2 constraint	ℓ_2 constraint	ℓ_2 constraint	embedding matrix ℓ_2 constraint	embedding matrix
# Negative Examples Per Positive Example in Training	1	chosen using validation set	1	as many as needed to find a violator	as many as needed to find a violator
Learning rate adaptation	adagrad	adagrad	adagrad	based on estimated rank	adagrad
Empirical Class Confusion Loss	no	no	no	no	yes
Discriminant Function $f_g(x)$	$\beta_g^T x$	$\beta_g^T x$	$\beta_g^T x$	$\beta_g^T W x$	$\|\beta_g - Wx\|_2^2$

Table 5: Comparison of the Different Stochastic Gradient Methods as Implemented in Experiments

The nearest means classifier is the most efficient to train of the compared methods as it only passes over the training samples once and computes the mean of the training feature vectors for each class (and there are no hyperparameters).

Like the nearest means classifier, we implemented Wsabie^{++} with Euclidean discriminants (as detailed in Table 3) and as such it can be considered a *discriminative* nearest means classifier. Testing with Euclidean discriminants can easily be made faster by applying exact or approximate fast k-NN methods, where the class prototypes $\{\beta_g\}$ play the role of the neighbors. Further, Euclidean discriminants lend themselves more naturally to visualization than the inner product, as each class is represented by a prototype.

One-vs-all linear SVMs are the most popular choice for large-scale classifiers due to studies showing their good performance, their parallelizable training, relatively small memory, and fast test-time (Rifkin and Klatau, 2004; Deng et al., 2010; Sanchez and Perronnin, 2011; Perronnin et al., 2012; Lin et al., 2011). Perronnin et al. (2012) highlights the importance of getting the right balance of negative to positive examples used to train the one-vs-all linear SVMs. As in their paper, we cross-validate the expected number of negative examples per positive example; the allowable choices were powers of 2. In contrast, earlier published results by Weston et al. (2011) that compared Wsabie to one-vs-all SVMs used one negative example per positive example, analogous to the AUC classifier. We included this comparison, which we labelled One-vs-all SVMs 1+:1- in the tables.

Both Wsabie and Wsabie^{++} jointly train an embedding matrix W as described in Section 3.5. The embedding dimension d was chosen on the validation set from the choices $d = \{32, 64, 96, 128, 192, 256, 384, 512, 768, 1024\}$ embedding dimensions. In addition, we created *ensemble* Wsabie and Wsabie^{++} classifiers by concatenating $\lfloor \frac{m}{d} \rfloor$ such d-dimensional models to produce a classifier with a total of m parameters to compare classifiers that require the same memory and test-time.

All hyperparameters were chosen based on the accuracy on a held-out validation set. Step-size, margin, and regularization constant hyperparameters were varied by powers of ten. The order Q of the last violators was varied by powers of 2. Chosen hyperparameters are recorded in Table 9. Both the pairwise loss and Wsabie classifier are implemented with standard ℓ_2 constraints on the class discriminants (and for Wsabie, on the rows of the embedding matrix). We did not use any regularization constraints for Wsabie^{++}.

We initialized the Wsabie parameters and SVM parameters uniformly randomly within the constraint set. We initialize the proposed training by setting all β_g to the origin, and all components of the embedding matrix are equally likely to be -1 or 1. Experiments with different initialization schemes for these different classifiers showed that different (reasonable) initializations gave very similar results.

With the exception of nearest means, all classifiers were trained online with stochastic gradients. We also used adagrad for the convex optimizations of both one-vs-all SVMs and the AUC sampling, which increased the speed of convergence.

Recently, Perronnin et al. (2012) showed good results with one-vs-all SVM classifiers and the WARP loss where they also cross-validated an early-stopping criterion. Adagrad reduces step sizes over time, and this removed the need to worry about early stopping. In fact, we did not see any obvious overfitting with any of the classifier training (validation set and test set errors were statistically similar). Each algorithm was allowed to train on up to 100 loops through the entire training set or until the validation set performance had

not changed in 24 hours. Even those runs that ran the entire 100 loops appeared to have essentially converged. Implemented in C++ without parallelization, all algorithms (except nearest means) took around one week to train the 16k Imagenet dataset, around two weeks to train the 21k and 22k datasets, and around one month to train the 97k dataset. Also in all cases roughly 80% of the validation accuracy was achieved in roughly the first 20% of the training time.

Because stochastic gradient descent uses random sampling of the training samples, multiple runs will produce slightly different results. To address this randomness, we ran five runs of each classifier for each set of candidate parameters, and reported the test accuracy and parameters for the run that had the best accuracy on the validation set. For one-vs-all SVMs with its convex objective, the five runs usually differed by .1% (absolute), whereas optimizing the nonconvex objectives of Wsabie and Wsabie^{++} produced much greater randomness within five runs, as much as .5% (absolute). Cross-validating between substantially more runs (e.g. 50 runs) of the training, would probably produce classifiers with slightly better accuracy, but cross-validating between too many runs could just lead to overfitting. We did not explore this issue carefully.

8.4 Metrics

Each classifier outputs the class it considers the one best prediction for a given test sample. We measure the accuracy of these predictions averaged over all the samples in the test set. For some datasets, such as the Web Datasets, samples may have more than one correct class, and are counted as correct if the classifier picks any one of the correct classes. Note that some results published for Imagenet use a slightly different metric: classification accuracy averaged over the G classes (Deng et al., 2010).

9. Results

We first give some illustrative results showing the effect of the three proposed differences between Wsabie^{++} and Wsabie. Then we compare Wsabie^{++} to four different efficient classifiers on four large-scale datasets.

9.1 Comparison of Different Aspects of Wsabie^{++}

Wsabie^{++} as detailed in Table 2 differs from the Wsabie classifier Weston et al. (2011) in the following respects:

1. ignores last violators
2. weights all stochastic gradients equally, that is, $w(r(y^+)) = 1$ in (11),
3. uses adagrad to adapt the learning rates,
4. uses Euclidean discriminants and no parameter regularization, rather than linear discriminants and ℓ_2 parameter regularization as done in Wsabie.

Table 6 shows how each of these first three differences increases the classification accuracy on the 21k Web dataset. For the results in this table, the embedding dimension was

Classifier	Test Accuracy
Wsabie (Weston et al., 2011)	3.7%
Wsabie + 10 last violators	5.0%
Wsabie + adagrad	5.0%
Wsabie + $w(r(y^+)) = 1$ in (11)	4.1%
Wsabie + adagrad + 10 last violators	5.9%
Wsabie + adagrad + $w(r(y^+)) = 1$ in (11)	6.0%
Wsabie + adagrad + $w(r(y^+)) = 1$ in (11) + 1 last violator	6.3%
Wsabie + adagrad + $w(r(y^+)) = 1$ in (11) + 10 last violators	7.1%
Wsabie + adagrad + $w(r(y^+)) = 1$ in (11) + 100 last violators	6.8%

Table 6: Effect of the proposed differences compared to Wsabie for a $d = 100$ dimensional embedding space on 21k Web Data.

fixed at $d = 100$, but all other classifier parameters were chosen to maximize accuracy on the validation set.

In addition, for simplicity we used Euclidean discriminants rather than linear discriminants: with Euclidean discriminants we found we did not need any additional parameter regularization, and it is simpler to apply adagrad when the parameters are unconstrained.

The results show that either adagrad or 10 last violators alone improves accuracy by 35%. Weighting all updates equally ($w(r(y^+)) = 1$) alone also improves accuracy by 10%. In combination, these changes complement each other, almost doubling the accuracy from 3.7% to 7.1%.

Table 7 gives examples of the classes corresponding to neighboring $\{\beta_g\}$ in the embedded feature space after the Wsabie^{++} training.

Lastly, we illustrate how the Wsabie^{++} test accuracy depends on the number of embedding dimensions. These results are for the 21k Web Dataset, with the step-size and margin parameters chosen using the validation set, and 10 last violators:

Number of Dimensions:	128	192	256	384	512	768	1024
Wsabie^{++} Test Accuracy:	7.4%	7.7%	8.3%	7.9%	7.1%	6.7%	6.5%

9.2 Comparison of Different Classifiers

Table 8 compares the accuracy of the different classifiers, where all hyperparameters were cross-validated. The validated parameter choices are reported in Table 9.[2]

Wsabie^{++} was consistently most accurate, followed by the one-vs-all SVMs with the average number of negative samples per positive sample chosen by validation. The row labelled Wsabie^{++} was $2-26\%$ more accurate and $2-4\times$ more efficient ($2-4\times$ smaller model size) than the one-vs-all SVMs because the validated embedding dimension was 192 or 256 dimensions, down from the original 479 or 1024 features.

2. Parameters for step-size and margin were not independent, with larger margins working better with larger step-sizes. We hypothesize that one of these parameters could be fixed and only the other cross-validated. We did not see any overfitting: scores on the validation set were statistically similar to scores on the test sets for all the compared methods.

Class	1-NN	2-NN	3-NN	4-NN	5-NN
poodle	caniche	pudel	labrador	puppies	cocker spaniel
dolphin	dauphin	delfin	dolfinjnen	delfiner	dolphins
San Diego	Puerto Madero	Sydney	Vancouver	Kanada	Tripoli
mountain	mountains	montagne	Everest	Alaska	Himalaya
router	modem	switch	server	lan	network
calligraphy	fonts	Islamic calligraphy	borders	quotes	network

Table 7: For each of the classes on the left, the table shows the five nearest (in terms of Euclidean distance) class prototypes $\{\beta_g\}$ in the proposed discriminatively trained embedded feature space for 21k Web Dataset. Because these classes originated as web queries, some class names are translations of each other, for example `dolphin` and `dauphin` (French for dolphin). While these may seem like exact synonyms, in fact different language communities often have slightly different visual notions of the same concept. Similarly, the classes `Obama` and `President Obama` are expected to be largely overlapping, but their class distributions differ in the formality and context of the images.

Like Perronnin et al. (2012), our experiments showed that choosing the hyperparameter of how many negative samples per positive sample for the one-vs-all SVMs made an impressive difference to its performance. The one-vs-all SVMs 1+:1-, which used a fixed ratio of one negative sample per positive sample was $2-4$ times worse!

The row labelled Wsabie^{++} Ensemble is a concatenation of 2-4 Wsabie^{++} classifiers trained on different random samplings so that the total number of parameters is roughly the same as the SVM (the embedding matrices W add slightly to the total storage and efficiency calculations). With efficiency thus roughly controlled, the accuracy gain increased slightly to $3-28\%$.

The least improvement was seen on the 21k Web Dataset. Our best hypothesis as to why that is that the classifiers are already close to the best performance possible with linear separators, and so there is little headroom for improvement. Some support for this hypothesis is the tiny gain the ensemble of multiple Wsabie^{++} classifiers versus the Wsabie^{++}.

One surprise was that Wsabie^{++} performed almost as well on the 97k Web Data as on the 21k Web Dataset even though there were four times as many classes. We have two main hypotheses of why this happened. First, there were more training samples in the 97k Web Data for the classes that were already present in the 21k Web Data. Second, the added classes had fewer samples but were often quite specific, and the samples from a specific class can be easier to distinguish than samples from a more generic class. For example, samples

from the more specific class of `diamond earrings` are easier to distinguish than samples from the more generic class `jewelry`. Likewise, samples from the class `beer foam` are easier to correctly classify than samples from the class `beer`.

	16k ImageNet	22k ImageNet	21k Web Data	97k Web Data
Nearest Means	4.4%	2.7%	2.6%	2.3%
One-vs-all SVMs 1+:1-	4.1%	3.5%	2.1%	1.6%
One-vs-all SVMs	9.4%	8.2%	8.3%	6.8%
AUC Sampling	4.7%	5.1%	2.8%	3.1%
Wsabie	6.5%	6.6%	4.5%	2.8%
Wsabie Ensemble	8.1%	7.0%	6.0%	3.4%
Wsabie^{++}	11.2%	10.3%	8.5%	8.2%
Wsabie^{++} Ensemble	**11.9%**	**10.5%**	**8.6%**	**8.3%**

Table 8: Image Classification Test Accuracy

10. Discussion, Hypotheses and Key Issues

This paper focused on how highly confusable classes can distort the empirical loss used in discriminative training of multi-class classifiers. We proposed a lightweight online approach to reduce the effect of highly-confusable classes on the empirical loss, and showed that it can substantially increase performance in practice. Experimentally, we also showed that using adagrad to evolve the learning rates in the stochastic gradient descent is effective despite the nonconvexity of the loss (due to the joint learning of the linear dimensionality reduction and linear classifiers).

We argued that when there are many classes it is suboptimal to measure performance by simply counting errors, because this overemphasizes the noise of highly-confusable classes. Yet our test error is measured in the standard way: by counting how many samples were classified incorrectly. A better approach to measuring test error would be subjective judgements of error. In fact, we have verified that for the image classification problems considered in the experiments, subjects are less critical about confusions of classes they consider more confusable (e.g. confusing `dolphin` and `porpoise`), but very critical of confusions between classes they do not consider confusable (e.g. `dolphin` and `Statue of Liberty`). Thus, suppose you had two candidate classifiers, each of which made 100 errors, but one made all 100 errors between `dolphin` and `porpoise` and the other made 100 more random errors. Standard test error of summing the errors would consider these classifiers equal, but users would generally prefer the first classifier. Weston et al. (2011) provide one approach to addressing this issue with a *sibling precision* measure.

A related issue is that it is known that the experimental datasets used are not tagged with the complete set of correct class labels for each image. For example, in the 21k Web Data, an image of a red heart might be labelled `love` and `red`, but not happen to be labelled `heart`, even though that would be considered a correct label in a subjective evaluation. We hypothesize that the proposed approach of probabilistically ignoring samples with consistent confusions helps reduce the impact of such missing positive labels.

	Stepsize	Margin	Embedding dimension	Balance β	# LVs
One-vs-all SVM 1+:1-					
16k ImageNet	.01	.1			
21k ImageNet	.01	.1			
21k Web Data	.1	1			
97k Web Data	.01	.1			
One-vs-all SVM					
16k ImageNet	.01	.1		64	
21k ImageNet	.01	.1		64	
21k Web Data	.1	1		64	
97k Web Data	.01	.1		128	
AUC Sampling					
16k ImageNet	.01	.1			
21k ImageNet	.01	.1			
21k Web Data	.001	.01			
97k Web Data	.001	.01			
Wsabie					
16k ImageNet	.01	.1	128		
21k ImageNet	.001	.1	128		
21k Web Data	.001	.1	256		
97k Web Data	.0001	.1	256		
Wsabie^{++}:					
16k ImageNet	10	10,000	192		8
21k ImageNet	10	10,000	192		8
21k Web Data	10	10,000	256		8
97k Web Data	10	10,000	256		32

Table 9: Classifier Parameters Chosen Using Validation Set

We built on WARP, which finds a violating class per each training sample if one exists. This strategy works much better in practice than the AUC sampling that samples one positive class and one negative class per training sample. We believe this is because WARP sampling focuses on improving the parameters of classes that are already quite good, rather than focusing on parameters for classes that are very confused. Analogously, and in agreement with results by Perronnin et al. (2012) on very different features, we saw that sampling one negative sample per positive sample for one-vs-all SVMs performed very poorly compared to sampling a validated number of negatives per positive. Inspired by these performance differences due to the choice of negative:positive ratios, we also considered validating a hyperparameter for Wsabie^{++} that would determine how many negative classes to consider for each positive class, rather than the WARP sampling which draws negative

classes until it finds a violator. Preliminary results showed that the validation set chose the largest parameter choice which was almost the same as the number of classes. Thus that approach required another hyperparameter but seemed to be doing exactly what WARP sampling does and appeared to offer no accuracy improvement over WARP sampling.

This research focused on accurate and efficient classification, and not on the issue of training time. With the exception of nearest means, the methods compared were implemented with stochastic gradient descent for efficient online training to deal with the large number of training samples n. As implemented, the methods took roughly equally long to train. However, parallel training of the G one-vs-all SVMs would have been roughly G times as fast. While not as naturally parallelizable, we have had some success in parallelizing the WARP sampling strategy across multiple cores and multiple machines, but the details are outside the scope of this work.

Our experiments were some of the largest image labeling experiments ever performed, and were carefully implemented and executed. But our experiments were narrow and limited in the sense that only image labeling problems were considered, and that the feature derivations were similar and all dense. The presented theory and motivation was not limited however, and we hypothesize that similar results would hold up for other applications, different features, and sparser features.

We focused in this paper only on classifiers that use linear (or Euclidean) discriminant functions because they are popular for large-scale highly multiclass problems due to their efficiency and reasonably good performance. However, for a given feature set, the best performance on large datasets such as ImageNet may well be achieved with exact k-NN (Deng et al., 2010; Weston et al., 2013b) or a more sophisticated lazy classifier (Garcia et al., 2010), or with a more flexible function class like that provided by a deep network (e.g. (Krizhevsky et al., 2012; Dean et al., 2012)) However, for many real-life large-scale problems these methods may require infeasible memory and test-time, and so linear methods are of interest at least for their efficiency, and may be used to filter candidates to a smaller set for secondary evaluation by a more flexible classifier. In addition, the last layer of a neural network is often a linear or other high-model-bias classifier, and the proposed approaches may thus be useful in training a deep network as well.

Label trees and label partitioning can be even more efficient at inference (Bengio et al., 2010; Deng et al., 2011; Weston et al., 2013a). We did not take advantage or impose a hierarchical structure on the classes, which can be a fruitful approach to efficiently implementing highly multiclass classification. Other research in large-scale classification takes advantage of the natural hierarchy of classes in real-world classification problems such as labeling images (Deng et al., 2010; Griffin and Perona, 2008; Nister and Stewenius, 2006). For example, in Web Data one class is `wedding cake`, which could fit into the broader class of `cake`, and the even broader class of `food`. One problem with leveraging such hierarchies may be that they are not strict trees; `wedding cake` also falls under the broader class of `wedding`, or there may be no natural hierarchy. Some of the theory and strategy of this paper should be complementary to such hierarchical approaches.

Acknowledgments

We thank Mouhamadou Cisse, Gal Chechik, Andrew Cotter, Koby Crammer, John Duchi, Bela Frigyik, and Yoram Singer for helpful discussions.

Appendix: Proof of Proposition 1

Let Z_t be a Bernoulli random variable with parameter p that models the event that the tth sample of class y^+ is classified as class h. Then for n trials the expected number of times a class y^+ sample is classified as class h is $E[\sum_t Z_t] = \sum_t E[Z_t] = nE[Z_t] = np$ the Z_t are independent and identically distributed.

Let O_t be another Bernoulli random variable such that $O_t = 1$ if the tth sample of class y^+ is counted in the loss given by (14), and $O_t = 0$ otherwise. Note that $O_1 = Z_1$, and for $t > 1$, $O_t = 1$ iff $Z_t = 1$ and $Z_{t-1} = 0$. Thus,

$$E[O_t] = E[Z_t = 1 \text{ and } Z_{t-1} = 0] = P(Z_t = 1, Z_{t-1} = 0) = P(Z_t = 1)P(Z_t = 0) = p(1-p)$$

by the independence of the Bernoulli random variables Z_t and Z_{t-1}. Then the expected number of confusions counted by (14) is $E[\sum_t O_t] = \sum_t E[O_t]$ by linearity, which can be expanded: $E[O_1] + \sum_{t=2}^{n} E[O_t] = p + (n-1)p(1-p)$.

References

E. L. Allwein, R. E. Schapire, and Y. Singer. Reducing multiclass to binary: a unifying approach for margin classifiers. *Journal Machine Learning Research*, 1:113–141, 2000.

A. Barla, F. Odone, and A. Verri. Histogram intersection kernel for image classification. *Intl. Conf. Image Processing (ICIP)*, 3:513–516, 2003.

S. Bengio, J. Weston, and D. Grangier. Label embedding trees for large multi-class tasks. In *NIPS*, 2010.

Y. Bengio. Learning deep architectures for AI. *Foundations and Trends in Machine Learning*, 2(1):1–127, 2009.

Y. Bengio, J. Laouradour, R. Collobert, and J. Weston. Curriculum learning. In *ICML*, 2009.

E. J. Bredensteiner and K. P. Bennet. Multicategory classification by support vector machines. *Computational Optimization and Applications*, 12:53–79, 1999.

L. D. Brown, T. T. Cai, and A. DasGupta. Interval estimation for a binomial proportion. *Statistical Science*, 16(2):101–117, 2001.

K. Crammer and Y. Singer. On the algorithmic implementation of multiclass kernel-based vector machines. *Journal Machine Learning Research*, 2001.

K. Crammer and Y. Singer. On the learnability and design of output codes for multiclass problems. *Machine Learning*, 47(2):201–233, 2002.

K. Crammer, O. Dekel, J. Keshet, S. Shalev-Shwartz, and Y. Singer. Online passive aggressive algorithms. *Journal Machine Learning Research*, 7:551–585, 2006.

A. Daniely, S. Sabato, and S. Shalev-Shwartz. Multiclass learning approaches: A theoretical comparison with implications. In *NIPS*, 2012.

J. Dean, G. S. Corrado, R. Monga, K. Chen, M. Devin, Q. V. Le, M. Z. Mao, M. Ranzato, A. Senoir, P. Tucker, K. Yang, and A. Ng. Large scale distributed deep networks. In *NIPS*, 2012.

J. Deng, W. Dong, R. Socher, L.-J. Li, K. Li, and L. Fei-Fei. ImageNet: A Large-Scale Hierarchical Image Database. In *IEEE Conf. Computer Vision Pattern Recognition (CVPR)*, 2009.

J. Deng, A. Berg, K. Li, and L. Fei-Fei. What does classifying more than 10,000 image categories tell us? In *European Conf. Computer Vision (ECCV)*, 2010.

J. Deng, S. Satheesh, A. C. Berg, and L. Fei-Fei. Fast and balanced: Efficient label tree learning for large scale object recognition. In *NIPS*, 2011.

T. G. Dietterich and G. Bakiri. Solving multiclass learning problems via error-correcting output codes. *Journal Artificial Intelligence Research*, 2:264–286, 1995.

J. Duchi, E. Hazan, and Y. Singer. Adaptive subgradient methods for online learning and stochastic optimization. *Journal Machine Learning Research*, 12:2121–2159, 2011.

D. Eck. Personal communication from Google music expert Douglas Eck. 2013.

C. Fellbaum, editor. *WordNet: An Electronic Lexical Database*. MIT Press, 1998.

E. K. Garcia, S. Feldman, M. R. Gupta, and S. Srivastava. Completely lazy learning. *IEEE Trans. Knowledge and Data Engineering*, 22(9):1274–1285, 2010.

D. Grangier and S. Bengio. A discriminative kernel-based model to rank images from text queries. *IEEE Trans. Pattern Analysis and Machine Intelligence*, 30:1371–1384, 2008.

K. Grauman and T. Darrell. The pyramid match kernel: Efficient learning with sets of features. *Journal Machine Learning Research*, 8:725–760, April 2007.

G. Griffin and P. Perona. Learning and using taxonomies for fast visual categorization. In *CVPR*, 2008.

Y. Guermeur. Combining discriminant models with new multi-class SVMs. *Pattern Analysis and Applications*, 5:168–179, 2002.

P. Hall and J. S. Marron. Geometric representation of high dimension, low sample size data. *J. R. Statst. Soc. B*, 67(3):427–444, 2005.

T. Hastie, R. Tibshirani, and J. Friedman. *The Elements of Statistical Learning*. Springer-Verlag, New York, 2001.

R. Herbrich, T. Graepel, and K. Obermayer. Large margin rank boundaries for ordinal regression. In *Advances in Large Margin Classifiers*, pages 115–132. MIT Press, 2000.

A. Krizhevsky, I. Sutskever, and G. E. Hinton. ImageNet classification with deep convolutional neural networks. In *NIPS*, 2012.

Y. Lee, Y. Lin, and G. Wahba. Multicategory support vector machines. *Journal American Statistical Association*, 99(465):67–81, 2004.

T. Leung and J. Malik. Recognizing surface using three-dimensional textons. *Intl. Conf. Computer Vision (ICCV)*, 1999.

Y. Lin, F. Lv, S. Zhu, M. Yang, T. Cour, K. Yu, L. Cao, and T. Huang. Large-scale image classification: Fast feature extraction and SVM training. In *CVPR*, 2011.

M. Mohri, A. Rostamizadeh, and A. Talwalkar. *Foundations of Machine Learning*. MIT Press, Cambridge, MA, 2012.

Y. Mroueh, T. Poggio, L. Rosasco, and J-J E. Slotine. Multiclass learning with simplex coding. In *NIPS*, 2012.

D. Nister and H. Stewenius. Scalable recognition with a vocabulary tree. In *CVPR*, 2006.

A. Paton, N. Brummitt, R. Govaerts, K. Harman, S. Hinchcliffe, B. Allkin, and E. Lughadha. Target 1 of the global strategy for plant conservation: a working list of all known plant speciesprogress and prospects. *Taxon*, 57:602–611, 2008.

F. Perronnin, Z. Akata, Z. Harchaoui, and C. Schmid. Towards good practice in large-scale learning for image classification. In *CVPR*, 2012.

R. Rifkin and A. Klatau. In defense of one-vs-all classification. *Journal Machine Learning Research*, 5:101–141, 2004.

J. Sanchez and F. Perronnin. High-dimensional signature compression for large-scale image classification. In *CVPR*, 2011.

B. Schoelkopf, A. J. Smola, and K. R. Müller. Kernel principal component analysis. *Advances in kernel methods: support vector learning*, pages 327–352, 1999.

O. Shamir and O. Dekel. Multiclass-multilabel classication with more classes than examples. In *Proc. AISTATS*, 2010.

A. Statnikov, C. F. Aliferis, I. Tsamardinos, D. Hardin, and S. Levy. A comprehensive evaluation of multicategory classification methods for microarray gene expression cancer diagnosis. *Bioinformatics*, 21(5):631–643, 2005.

A. Tewari and P. L. Bartlett. On the consistency of multiclass classification methods. *Journal Machine Learning Research*, 2007.

N. Usunier, D. Buffoni, and P. Gallinari. Ranking with ordered weighted pairwise classification. In *ICML*, 2009.

V. Vapnik. *Statistical Learning Theory*. 1998.

J. Weston and C. Watkins. Multi-class support vector machines. *Technical Report CSD-TR-98-04 Dept. Computer Science, Royal Holloway, University London*, 1998.

J. Weston and C. Watkins. Support vector machines for multi-class pattern recognition. In *Proc. European Symposium on Artificial Neural Networks*, 1999.

J. Weston, S. Bengio, and N. Usunier. Wsabie: Scaling up to large vocabulary image annotation. In *Intl. Joint Conf. Artificial Intelligence, (IJCAI)*, pages 2764–2770, 2011.

J. Weston, A. Makadia, and H. Yee. Label partitioning for sublinear ranking. In *ICML*, 2013a.

J. Weston, R. Weiss, and H. Yee. Affinity weighted embedding. In *Proc. International Conf. Learning Representations*, 2013b.

L. Xiao. Dual averaging methods for regularized stochastic learning and online optimization. *Microsoft Research Technical Report MSR-TR-2010-23*, 2010.

T. Zhang. Statistical analysis of some multi-category large margin classification methods. *Journal Machine Learning Research*, 5:1225–1251, 2004.